REPORT DOCUMENTATION PAGE

Form Approved
OMB No. 0704-0188

1. AGENCY USE ONLY (Leave blank)	2. REPORT DATE	3. REPORT TYPE AND DATES COVERED
	1/11/95	Final Technical 7/31/94 -10/1/95

4. TITLE AND SUBTITLE
Robust Inversion Methods for Problems in LDV and SAW

5. FUNDING NUMBERS
G
N00014-94-1-1165

6. AUTHOR(S)
Richard Barakat

7. PERFORMING ORGANIZATION NAME(S) AND ADDRESS(ES)
Tufts University
Grants & Contracts Administration
Packard Hall
Medford, MA 02155

8. PERFORMING ORGANIZATION REPORT NUMBER

9. SPONSORING/MONITORING AGENCY NAME(S) AND ADDRESS(ES)
Office of Naval Research
495 Summer Street, Room 103
Boston, MA 02210

10. SPONSORING/MONITORING AGENCY REPORT NUMBER

11. SUPPLEMENTARY NOTES

12a. DISTRIBUTION/AVAILABILITY STATEMENT
Approved for public release; distribution is unlimited.

12b. DISTRIBUTION CODE

13. ABSTRACT *(Maximum 200 words)*

See attached.

14. SUBJECT TERMS
Saw velocity fluctuation analysis, surface acoustic waves
laser doppler velociemetry

15. NUMBER OF PAGES
50

16. PRICE CODE

17. SECURITY CLASSIFICATION OF REPORT	18. SECURITY CLASSIFICATION OF THIS PAGE	19. SECURITY CLASSIFICATION OF ABSTRACT	20. LIMITATION OF ABSTRACT
Unclassified	unclassified	unclassified	UL

DISCLAIMER NOTICE

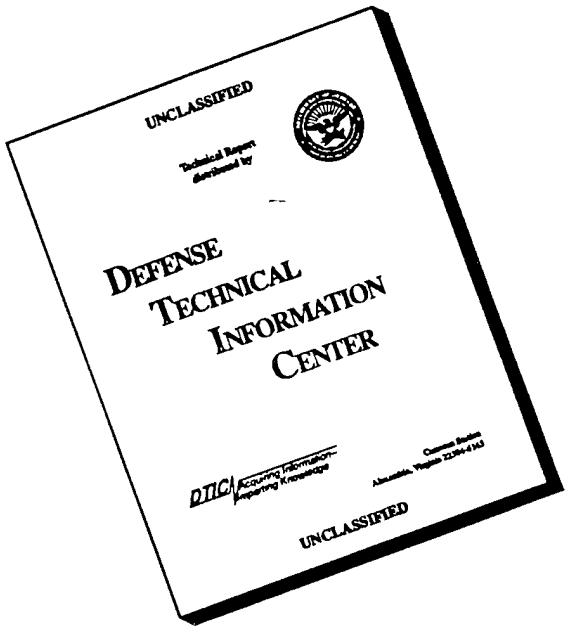

THIS DOCUMENT IS BEST QUALITY AVAILABLE. THE COPY FURNISHED TO DTIC CONTAINED A SIGNIFICANT NUMBER OF PAGES WHICH DO NOT REPRODUCE LEGIBLY.

DECONVOLUTION ASPECTS OF SAW

AND

VELOCITY FLUCTUATION ANALYSIS OF LDV

Report to:

Office of Naval Research
Dr. William Stachnik

N00014-94-1-1165

Richard Barakat
Electro-Optics Technology Center
Tufts University
Medford, MA 02155

1 November 1995

INTRODUCTION

The technical content of the research carried out under the aegis of this contract is covered under two essentially distinct topics:

A. Inversion problems associated with surface acoustic waves (SAW)

B. Inversion problems associated with laser doppler velocimetry (LDV); signal-to-noise issues occurring in LDV.

These two topics will be discussed separately.

We should point out that no attempt was made to provide detailed numerical results as has been my custom for the last thirty years. The reasons are two-fold: firstly, these two topics do not lend themselves to a numerical description in terms of a few parameters (especially LDV) so that really detailed parameter calculations must be carried (it is my feeling that a limited parameter series of calculations will probably lead to such an incomplete numerical description that false "rule-of-thumb" conclusions may be drawn); secondly, the mathematical description of both topics leads to nonlinear mathematical operations that are just too complicated (and require enormous memory) to be run on workstations of even VAXs, we need massively parallel computing power to effect the numerical calculations such as a CONNECTION machine or the new IBM parallel machine on MAUI. Nevertheless numerical computations were carried out on a VAX to illustrate some aspects of topic A.

NUMERICAL INVERSION OF NONLINEAR INTEGRAL EQUATIONS OF THE FIRST KIND WITH APPLICATIONS TO SURFACE ACOUSTIC WAVE PROBLEMS

The second topic: inversion of nonlinear integral equations of the first kind with applications to SAW (surface acoustic waves), has been treated in a quite general manner concentrating upon the development of an algorithm that is reasonably robust with respect to measurement noise. The technique developed depends upon a relatively new idea, that of "trust regions", in conjunction with Newton-like methods which involve exact calculations of both Jacobian and Hessians of the least squares objective function. The necessary reasons for using this approach (as well as the mathematical) are worked out and discussed in the main text of this section. Rather than attempting the inversion problem in the context of SAW, I have decided to cast the specifics in terms of a formally similar problem: "inversion of the modulus/phase of a coherently illuminated object from its measured diffraction image" as I have worked extensively in the area of optical diffraction theory with the result that I have a good heuristic feeling for the plausibility of the correctness of the "solution". I am now confident of the usefulness of the proposed algorithm having run some numerical inversions (see main text). It is now a straightforward matter to transform the algorithm specifics into the SAW inversion problem in accordance with information to be provided by Dr. W. Micelli.

As noted in the last paragraph of page 20, a constrained version of the problem has been developed in order to handle (if necessary) the non-negativity of the solution. Further, as noted at the end of page 8, we really need to use a parallel machine (such as on Maui) if we are going to speed up the calculations for the SAW problem. The calculations presented here were carried out on a VAX, a truly slow machine by todays standards.

ABSTRACT

An algorithm for recovering the modulus and phase of a coherently illuminated object from its measured diffraction image is presented. The algorithm is based upon the fact that both the Jacobian and Hessian matrices can be evaluated exactly so that both slope and curvature information is available. The inversion problem is cast as a nonlinear unconstrained optimization problem, and trust region techniques are employed for its solution. Representative numericals are presented.

1. INTRODUCTION

The problem of measuring the diffraction image of an incoherently illuminated object and working back to determine (or estimate) the object itself has been of great interest in many scientific and technical areas for the past twenty years. The subject has grown to such an extent that even listing the books and major review articles is a tedious undertaking.

At the other extreme, we have the analogous problem for a coherently illuminated object, a much more difficult problem because the relation between object and diffraction image is nonlinear, whereas the corresponding relation for incoherently illuminated objects is linear. In many respects the coherently illuminated situation is much older than the incoherently illuminated situation in that light microscopists have always encountered such problems. Their "solutions" have generally been of the old-fashioned expert systems type; they have encountered over the years a variety of biological objects and developed an empirical expertise in sorting out situations. In a sense their primary artifact is the diffraction image, not eh actual object, as witness the various phase contrast methods [1,2]. Unlike the incoherent situation, there is no guarantee that the topology of the object bears any resemblance to its coherent diffraction image. As an example, see Figure 1 which shows the diffraction image of an edge viewed through an optical system with an annular aperture [3].

In the present paper, a solution for the modulus and phase of a coherently illuminated object is obtained via a nonlinear regularized minimization algorithm. We have brought to bear powerful tools recently developed in numerical analysis (particularly trust region considerations) toward the efficient solution of the inversion problem. The present scheme takes advantage of the fact that we can evaluate both Jacobian and Hessian matrices *exactly*, thereby allowing use of slope and curvature information explicitly. There is no need to make the usual small residual approximation of the Hessian with its convergence limitation in the presence of measurement noise. A second benefit of knowing the Jacobian and Hessian explicitly is that we can make very efficient use of the trust region tests in determining the pat to local minima. There are a number of algorithms for the inversion of modulus/phase of coherently illuminated objects already published; see Stark [4] for an extremely useful summary. Practically all these algorithms will yield a reasonably accurate estimate of the support of the object, and the present algorithm is no exception. However, many coherently illuminated objects contain changes in modular/phase over the surface so that an algorithm (such as the one discussed here) which also can deliver information on the distribution of modulus/phase over the object is extremely useful for applications (e.g., biological light microscopy). Furthermore, the present method is reasonably robust with respect to noise because we operate in the large residual regime.

2. DIFFRACTION MODEL

The diffraction image of a coherently illuminated object, $I(x,y)$ in the image receiving plane with coordinates x, y is measured over a square lattice of points x_m, y_n:

$$\begin{matrix} x_m = \beta_m \\ y_n = \beta_n \end{matrix} \qquad m,n = 0, \pm 1, \pm 2, \ldots, \pm M \tag{2.1}$$

where β is a numerical constant. It is assumed that M is large enough for

$$I(x_{|M|}, y_{|M|}) \approx 0 \quad . \tag{2.2}$$

In what follows, it will be convenient to write $(x_m, y_m) \equiv h_{mn}$ as a column vector $\mathbf{I}$ of length $\widetilde{m} \equiv (2M+1)^2$ using standard Fortran lexiographic ordering.

We assume that the measured diffraction image can be modelled via scalar optical diffraction theory so that the model diffraction image, $\mathcal{I}(x,y)$, is given by the convolution

$$\mathcal{I}(x,y) = \left| \int\int_{\text{object}} a(x-x', y-y') o(x', y')\, dx' dy' \right|^2 \tag{2.3}$$

assuming the isoplanatic condition to hold.

The coherently illuminated object is characterized by a complex-valued function $o(x,y)$ with modulus $|o(x,y)|$ and phase $\arctan[o_i(x,y)/o_n(x,y)]$. The function $a(x,y)$ is the coherent point-spread function of the optical system performing the imaging; to within multiplicative factors it is

$$a(x,y) = \int\int_{\text{exit pupil}} A(\zeta,\eta) e^{i\frac{k}{f}(x\zeta + y\eta)} d\zeta d\eta \tag{2.4}$$

with k as the mean wavenumber of the coherent light and f the focal length. The pupil function $A(\zeta,\eta)$ is given by

$$A(\zeta,\eta) = B(\zeta,\eta)e^{ikW(\zeta,\eta)} \tag{2.5}$$

with $W(\zeta,\eta)$ the wavefront aberration function over the exit pupil and $B(\zeta,\eta)$ the amplitude distribution over the exit pupil; both are assumed known in the present scenario.

For the very important case of a circular aperture exit pupil of radius α for which $B(\zeta,\eta) = 1$ and $W(\zeta,\eta) = 0$, we have

$$a(x,y) = \frac{2J_1\left[\frac{k\alpha}{f}(x^2+y^2)^{1/2}\right]}{\left[\frac{k\alpha}{f}(x^2+y^2)^{1/2}\right]} \quad . \tag{2.6}$$

Since in most applications, the exit pupil is circular; under these circumstances it is convenient to employ normalized coordinates:

$$\begin{aligned} u &\equiv \frac{k\alpha}{f}x\,, \qquad v \equiv \frac{k\alpha}{f}y \\ p &= \frac{\zeta}{\alpha}\,, \qquad q = \frac{\eta}{\alpha} \end{aligned} \tag{2.7}$$

Consequently Eqs. (2.3), (2.4), and (2.6) become

$$\mathcal{I}(u,v) = \left| \iint\limits_{\text{object}} a(u-u',v-v')o(u',v')\,du'dv' \right|^2 \tag{2.3a}$$

$$a(u,v) = \iint\limits_{0\le p^2+q^2\le 1} A(p,q)e^{i(up+vq)}\,dpdq \tag{2.4a}$$

$$a(u,v) = \frac{2J_1((u^2+v^2)^{1/2})}{(u^2+v^2)^{1/2}} \tag{2.6a}$$

Leaving aside the mathematical details for the moment, let us consider the task before us. We are given *measured* values of the diffracted intensity and are required to determine the modulus and phase of the object assuming that the measured diffracted intensity can be modeled as the convolution, Eq. (2.3), and that we know the parameters of the optical system characterizing the coherent point spread function, Eq. (2.4). Said object is contained in the integrand of a double integral which is itself squared. When viewed from this perspective, we should not be unduly optimistic about achieving an accurate solution because of the inherent nonlinearity and strong smoothing action of the double integral. Irrespective of the actual inversion method, the strong smoothing action of the integration means that much high frequency data is lost and cannot be retrieved, even in principle. Only a low frequency version of the object can be obtained. Perhaps the best way to consider the problem is to interpret it thusly: we are given the "answer" ($\equiv$ effect) in the form of a noisy diffraction image of the object and are attempting to determine the "question" ($\equiv$ cause), the coherently illuminated object. The mathematical relation between answer and question is highly nonlinear by virtue of Eq. (2.2), bearing in mind that $a(u, v)$ is additionally an oscillating, complex-valued function.

In a sense this problem can be considered as a two-dimensional phase retrieval problem, see [5-11] for various details. We will not discuss the general issues of ill-posed inverse problems and refer the reader to [12,13] for *some* of the theoretical aspects.

Our diffraction model image $\mathcal{I}(u, v)$ is to be determined by the values of the image at the lattice points (u'_k, v'_ℓ) inside a square in the (u', v') plane that is large enough to contain the image. The number of object values, $o(v'_k, v'_\ell) \equiv o_{k\ell}$ is taken to be N. It is important to remember that both modulus and phase must be determined at each of these lattice points. Let $\tilde{n}$ be the number of unknown modulus and phase values (obviously $\tilde{n}$ must be even); the unknown $o_{k\ell}$ are to be written as a column vector $\mathbf{o}$.

Although we have run several dozen inversions, we do not possess a sufficiently large base to estimate benchmark performance. However, many of our inversions, regardless of the initial guess, took 150–180 iterates to converge. In a few cases, convergence was achieved in half this number; nevertheless we also encountered some cases where convergence required 200 iterations.

Generally the algorithm performance decomposed into two stages: (a) the initial stage wherein the objective functions went through wild gyrations in magnitude as the trust region subalgorithm had to compute many new gradient and Hessian matrices while searching for an appropriate direction of descent; (b) the second stage, when the trust region subalgorithm has locked into a subset of "optimal" directions of descent, the objective function then undergoes a monotone decrease to zero as the number of iterations is increased. We again warn the reader that although convergence is attained, there is no guarantee that the global minimum has been achieved.

As a final remark, we note that as the analysis is heavily dependent upon linear algebra (matrices, vectors); it would be of some interest to consider doing calculations via parallel processing algorithms to speed up the computations even more.

In this notation Eq. (2.3a) becomes $\mathcal{I}(\mathbf{o})$ where $\mathcal{I}$ is a vector of length $\tilde{m}$. The inversion problem relates the unknown (complex-valued) object values $\mathbf{o}$ of the assumed diffraction model to the measured diffraction image I via the nonlinear relation

$$\mathbf{I} = \mathcal{I}(\mathbf{o}) \quad . \tag{2.7}$$

This equation is to be interpreted as a system of $\tilde{m}$ nonlinear equations in $\tilde{n}$ unknowns. Enough data must be given to allow some smoothing of the measured diffraction image data as regards the diffraction model; consequently we let $\tilde{m} > \tilde{n}$ so that the nonlinear system is overdetermined. The problem now reduces to the solution of Eq. (2.7) in some normed sense.

It is of some interest to contrast the differences between the incoherently illuminated and coherently illuminated object situations. The relation between object and image for incoherently illuminated objects, again assuming that the isoplanatic conditions holds, is

$$I_i(x,y) = \int\int_{\text{object}} t(x-x', y-y') o_i(x',y')\, dx'dy' \tag{2.8}$$

where

$o_i(x,y) =$ intensity distribution over the
incoherently radiating object

$t(x,y) \propto |a(x,y)|^2 =$ incoherent point-spread function

$I_i(x,y) =$ intensity distribution over the diffraction
image of $o_i(x,y)$

Two points to note: (1) all functions in Eq. (2.8) are real and nonnegative, (2) the relation between answer, $I_i(x,y)$, and question, $o_i(x,y)$, is linear. On the other hand, for the coherently illuminated object only the diffracted intensity is real and nonnegative. Furthermore the relation between $I(x,y)$ and $o(x,y)$ is nonlinear. Consequently the incoherently illuminated object scenario is much easier to invert than the coherently illuminated object scenario.

3. PRELIMINARIES

In order to proceed, we next discretize the double integral on the right-hand side of Eq. (2.3a)

$$\mathcal{I}(u_m, v_m) \equiv \mathcal{I}_{mn} = \left| C \sum_{k=1}^{N} \sum_{\ell=1}^{N} \alpha_k \alpha_\ell a(u_m - u_k, v_n - v_\ell) o(v_k, v_\ell) \right|^2 \tag{3.1}$$

Here u_k, v_ℓ are the quadrature points and α_k, α_ℓ are the corresponding weight factors.

In the numerical algorithm we employ for the inversion (see next section), we require the first and second derivatives of $\mathcal{I}_{mn}$ with respect to $o_{k\ell}$ in order to form Jacobian and Hessian matrices. We need not write out the explicit formulas because we employed a symbol manipulation program (MAPLE) to evaluate them directly in the computer from which numerical values are obtained internally.

4. OUTLINE OF SOLUTION APPROACH

We now outline the *general* features of our numerical approach to the nonlinear phase retrieval problem via regularized unconstrained minimization. Our version of the unconstrained minimization problem is that of finding the least value of an objective function, $\epsilon(\mathbf{o})$. The term unconstrained indicates that the variables $\mathbf{o}$ are not limited in any way. In our application, we wish to determine a global minimum of ϵ, i.e., a point $\mathbf{o}^*$ satisfying

$$\epsilon(\mathbf{o}) \geq \epsilon(\mathbf{o}^*), \qquad \forall \mathbf{o} \quad . \tag{4.1}$$

Unfortunately we must be content with a local minimum:

$$\epsilon(\mathbf{o}) \geq \epsilon(\mathbf{o}^*) \qquad \forall \mathbf{o} \text{ , in a neighborhood of } \mathbf{o}^* \quad . \tag{4.2}$$

Solution of the global minimum problem is far harder than the solution of the local minimum problem which itself is extremely complicated [16,17].

The derivation of nearly all methods for unconstrained minimization is founded on the assumption that the objective function $\epsilon(\mathbf{o})$ can be approximated by a quadratic function in the neighborhood of a minimum point. Thus methods are sought which efficiently minimize quadratic functions in the hope that they will also be effective on more general functions, at least in the neighborhood of a minimum. When first and second derivatives of $\epsilon(\mathbf{o})$ are known, such as in our case, then we can make use of both gradient and curvature information to effect a solution. Furthermore, both gradient and curvature, as governed by $\mathbf{G}$ and $\mathbf{H}$, see Eqs. (4.4) and (4.5), can be calculated ***exactly*** in the context of the discretized version of our problem. Thus, we can avoid many of the difficulties associated with situations where $\mathbf{G}$ and $\mathbf{H}$ are known only approximately. The Taylor series expansion of the objective function can be used to approximate its minimum value from points $\mathbf{o}$ near to the minimum $\mathbf{o}^*$ by moving in a direction $\Delta\mathbf{o}$

$$\epsilon(\mathbf{o} + \Delta\mathbf{o}) \approx \epsilon(\mathbf{o}) + \mathbf{G}^T(\mathbf{o})(\Delta\mathbf{o}) + \frac{1}{2}(\Delta\mathbf{o})^T\mathbf{H}(\mathbf{o})(\Delta\mathbf{o}) \tag{4.3}$$

G and H are the gradient vector and Hessian matrix of the objective function, respectively

$$\mathbf{G}^T \equiv \left| \frac{\partial \epsilon}{\partial o_1}, \frac{\partial \epsilon}{\partial o_2}, \cdots, \frac{\partial \epsilon}{\partial o_{\tilde{n}}} \right| \tag{4.4}$$

$$\mathbf{H} \equiv \begin{vmatrix} \frac{\partial^2 \epsilon}{\partial o_1^2} & \cdots & \frac{\partial^2 \epsilon}{\partial o_1 \partial o_{\tilde{n}}} \\ \vdots & & \vdots \\ \frac{\partial^2 \epsilon}{\partial o_{\tilde{n}} \partial o_1} & \cdots & \frac{\partial^2 \epsilon}{\partial o_{\tilde{n}}^2} \end{vmatrix} \tag{4.5}$$

Note that H is symmetric. Both G and H are exact within the context of the discretization. The strategy is to determine the vector $\Delta \mathbf{o}$ of the movements required to approximate the minimum from the current point o.

Before proceeding further, it is important to state the conditions for a given point o to be an unconstrained strong minimum $\mathbf{o}^*$ (i.e., a point $\mathbf{o}^*$ for which the objective function increases locally in all directions. The first order necessary condition is [16,17]

$$\mathbf{G}(\mathbf{o}^*) = 0 \quad . \tag{4.6}$$

However, this condition is not sufficient as other types of minima (stationary points) also satisfy this condition. The second order condition follows from Eq. (4.2) and is [11,12]

$$(\Delta \mathbf{o})^T \mathbf{H}(\mathbf{o}^*)(\Delta \mathbf{o}) > 0 \tag{4.7}$$

which is sufficient to ensure that $\epsilon(\mathbf{o}^* + \Delta \mathbf{o}) > \epsilon(\mathbf{o}^*)$. If $\epsilon(\mathbf{o}) \neq 0$, this implies that $\mathbf{H}(\mathbf{o}^*)$ is a positive definite matrix. Therefore the second-order sufficient condition for a strong minimum is that $H(\mathbf{o}^*)$ should be positive definite.

Returning to Eq. (4.3), hereafter termed the local model of the object function, we initiate a search for $\mathbf{o}^*$ by moving $\Delta \mathbf{o}$. This involves an iterative procedure in that we

start from some point o and choose in some fashion a direction Δo in which the minimum is assumed to lie. This is repeated until the minimum is achieved (if possible). Because we are employing a quadratic version of $\epsilon(o)$ then the local model of $\epsilon(o)$ always allows us to find a solution. However, the local model of $\epsilon(o)$ is certainly not a useful approximation to $\epsilon(o)$ itself except near a minimum. It is an act of faith that the local model and the actual model are "close" in the vicinity of the minimum. Simple calculations [14,15] show that at a minimum

$$\Delta o = -[H(o)]^{-1} G(o) \quad . \tag{4.8}$$

This equation represents the appropriate direction Δo to take to the minimum o^*, based upon information at o. This equation is fundamental to all second-order minimization algorithms (i.e., algorithms employing both G and H). However, on the actual objective function surface, such as we are faced with, the local model of $\epsilon(o)$ is only accurate in the *immediate* vicinity of the minimum. This means that H may not be positive definite, as required by Eq. (4.7), since it is evaluated at points other than the minimum. This situation is most likely to occur at some distance from the minimum (i.e., for initial iterations) since at a point close to the minimum all sufficiently differentiable functions tend to behave as a quadratic function as their third and higher order derivatives in the Taylor series become negligible. We will return to the necessity of keeping H positive definite very shortly.

The classic approach to limiting step size during the iteration is a line search [14,15]. In line search tactics we compute a descent direction and subject this direction (which is generally not toward the unconstrained minimum) to a minimization procedure of which details can be found in the above references. Should the descent direction satisfy these criteria, this iteration is then terminated. We then repeat the process, etc. The difficulty of practical implementation is two-fold. First, such calculations are prohibitively expensive and the minimization criteria are therefore only approximate to save computer time;

yet they must be made precise enough to ensure reasonably quick convergence. Second, fulfilling these contradictory goals is something of a black art and the programming effort is very substantial, often occupying up to two-thirds of the coding for the entire optimization. For small problems, such as the slit aperture, line search methods are very useful and were employed along with regularized singular value decomposition in [18].

Although it is possible to use line search methodology for the 2-D aperture, we have chosen to employ a relatively new method which offers many advantages over the line search methodology, the trust region tactic [14-16]. A particular advantage of the trust region approach is in the very strong global convergence properties which hold with no significant restrictions on the class of problems to which they apply making it especially useful for the nonlinear minimization of phase retrieval in two dimensions. In addition, the trust region philosophy requires less computation than does the line search philosophy in terms of gradient and Hessian, but more computations have to be performed on the local model of the objective function.

Suppose we are at point $\mathrm{o}^{(k)}$, after the k-th iteration. Now let us *assume* that there is a region $\Delta^{(k)}$, which we take to be in the shape of a sphere of radius $h^{(k)}$

$$\Delta^{(k)} = \{\mathrm{o} : \|\mathrm{o} - \mathrm{o}^{(k)}\| \leq h^{(k)}\} \tag{4.9}$$

in which the local model of $\epsilon(\mathrm{o})$, given by the Taylor series Eq. (4.2) agrees with the actual objective function in some sense. One's obvious choice is to let

$$\mathrm{o}^{(k+1)} = \mathrm{o}^{(k)} + \Delta^{(k)} \tag{4.10}$$

where the correction $\Delta^{(k)}$ minimizes the local model (Δ) for all values of $\mathrm{o}^{(k)} + \Delta$ in $\Lambda^{(k)}$. An iteration step in o is to be restricted by the region of validity of the Taylor series. Thus we compute the gradient and Hessian, G and H, appropriate to $\mathrm{o}^{(k)}$ and minimize the

local model of $\epsilon(\mathrm{o})$ in order to determine the radius $h^{(k)}$ of the trust region. In formal language, we seek the solution of the problem

$$\text{minimize (local model) subject to constraint } \|\Delta\|_2 \leq h^{(k)} \ . \tag{4.11}$$

Before we can solve this subproblem it is necessary to choose some reasonable criterion on the radius $h^{(k)}$ of the trust region. Obviously, the criterion should not present undue restrictions, so that $h^{(k)}$ should be as large as possible subject to some agreed-upon idea as to the degree of closeness of the local model of $\epsilon(\mathrm{o})$ and $\epsilon(\mathrm{o})$. One way is to define the quality coefficient

$$r_k \equiv \frac{\epsilon(\mathrm{o}^{(k)} + \Delta^{(k)}) - \epsilon(\mathrm{o}^{(k)})}{\epsilon_q(\mathrm{o}^{(k)} + \Delta^{(k)}) - \epsilon_q(\mathrm{o}^{(k)})} \tag{4.12}$$

where the denominator is the predicted reduction of the local model of ϵ, now call it ϵ_q, while the numerator represents the reduction in the actual objective function. The closer r_k is to unity, the better the agreement between ϵ and ϵ_q. As a stopping criterion stop if $r_k > .8$ and go to the next iteration. If $r_k < .8$ reduce $h^{(k)}$ and repeat the calculation. The literature contains other stopping criteria but the one quoted above seems adequate for our purposes. See the quoted references for more details.

Thus far we have outlined the general features of the inversion problem, estimating o via minimization of an objective function ϵ, as yet unspecified. We feel that there are two objective functions of possible interest. The first is the usual least squares (L_2 norm) objective function

$$\epsilon(\mathrm{o}) = \sum_{i=1}^{\bar{m}} (\mathcal{I}_i - I_i)^2 \quad . \tag{4.13}$$

In this version of the problem, we consider the estimation of o via an (unconstrained) nonlinear least squares minimization. A second objective function is for an L_1 norm

$$\epsilon(\mathrm{o}) = \sum_{i=1}^{\bar{m}} |\mathcal{I}_i - I_i)| \tag{4.14}$$

Consequently we have allowed considerable flexibility in the ϵ minimization algorithm so as to accommodate both objective functions as well as others that may arise. For the purposes of the present paper, we confine the discussion to the L_2 norm aspects.

Upon defining the vector

$$\Phi(\mathrm{o}) = \mathcal{I} - \mathrm{I} \tag{4.15}$$

which is of length $\widetilde{m}$, we can rewrite Eq. (4.13) as

$$\epsilon(\mathrm{o}) = \Phi^T(\mathrm{o})\Phi(\mathrm{o}) \quad . \tag{4.16}$$

The elements of G and H can be expressed directly in terms of the elements Φ by introducing an ancillary matrix J given by

$$\mathrm{J} \equiv \begin{vmatrix} \frac{\partial \phi_1}{\partial o_1} & \cdots & \frac{\partial o_1}{\partial o_{\tilde{n}}} \\ \vdots & & \vdots \\ \frac{\partial \phi_{\widetilde{m}}}{\partial o_1} & \cdots & \frac{\partial \phi_{\widetilde{m}}}{\partial o_{\tilde{n}}} \end{vmatrix} \tag{4.17}$$

This matrix is generally rectangular. Thus

$$\frac{\partial \epsilon}{\partial o_j} = 2 \sum_{i=1}^{\widetilde{m}} \phi_i \frac{\partial \phi_i}{\partial o_j} \tag{4.18}$$

or

$$\mathrm{G} = 2\mathrm{J}^T\Phi \quad . \tag{4.19}$$

The corresponding elements of H are

$$\frac{\partial^2 \epsilon}{\partial o_k \partial o_\ell} = 2 \sum_{i=1}^{\widetilde{m}} \frac{\partial \phi_i}{\partial o_k} \frac{\partial \phi_i}{\partial o_\ell} + 2 \sum_{i=1}^{\widetilde{m}} \phi_i \frac{\partial^2 \phi_i}{\partial o_k \partial o_\ell} \tag{4.20}$$

with $k, \ell = 1, 2, \ldots, \tilde{n}$. The first term on the right-hand side is $2\mathrm{J}^T\mathrm{J}$ and we will call the second term S; thus

$$\mathrm{H} = 2\mathrm{J}^T\mathrm{J} + \mathrm{S} \tag{4.21}$$

There is no guarantee that H will always be positive definite through the calculations; in fact H will become almost singular as we approach the strong minimum. To avoid this state of affairs, we consider a regularized version of H. In the regularized version, we replace H by $\mathrm{H} + q\mathrm{I}$ where q, the regularizing parameter, is a small nonnegative real number. This procedure can remove H from near singularity and for sufficient large q restore the positive definite character of the Hessian. In linear problems, there is a well established method to estimate q [12]. In the nonlinear problem we employed q in the range $0.01 \leq q \leq 0.05$. There was not much difference in the final answers as long as $q > 0$; but setting $q = 0$ caused considerable numerical instability as expected.

5. A NUMERICAL EXAMPLE

It is not our intention to present a catalog of numerical results at this time, yet we wish to discuss the numerical workings of the algorithm in the presence of "measurement" noise. To this end we considered a known object $o(u,v)$ and from it calculated the diffraction image $\mathcal{I}(u,v)$ from Eq. (2.3a) using the point-spread function $a(u,v)$ corresponding to an in-focus, aberration-free optical system as given by Eq. (2.6a). The *measured* diffraction image $I(u,v)$ was taken to be given by

$$I(u,v) = [1 + \delta\mu(u,v)]\mathcal{I}(u,v) \tag{5.1}$$

where δ is a positive constant less than unity and $\mu(u_m, v_n)$ is a random variable uniformly distributed over $(-1,+1)$:

$$\begin{aligned} f(\mu) &= \frac{1}{2}\,, & |\mu| < 1 \\ &= 0\,, & |\mu| > 1 \end{aligned} \tag{5.2}$$

Values of δ used in the present calculations, such as $\delta = 0.04$ are described loosely as 4% a noise. Note that the noise we are introducing is intensity dependent noise; it is not intended to faithfully simulate actual detector noise but rather to mimic such noise for the purpose of testing the robustness of the inversion algorithm.

We have chosen the following lone object to illustrate the calculations:

$$\begin{aligned} o(u,v) &= 0\,, \qquad , & -\infty < v < -15 \\ &= \frac{3}{8}[3 + \mathrm{erf}(v)]\,, & -15 < v < 15 \\ &= 0\,, & -15 < v < \infty \end{aligned} \tag{5.3}$$

where $\mathrm{erf}(v)$ is the error function. There are two reasons for choosing this object. The first reason is that the modulus of the object exhibits a spatial variation. One of the

(as yet unstated) requirements on the algorithm is that it be able to recover reasonably accurate estimates of the object photometry in addition to estimating its size; as noted in the introduction almost any of the currently available algorithms can perform this; very few seem to be able to provide reasonably accurate estimates of photometry. The second reason for choosing this object is that it is very small in width being slightly less than Airy disk radius across (recall that an Airy disk radius ≈ 3.82). These two constraints present a severe test of the algorithm.

Calculations were run for the *completely unrealistic* case of the noise-free, measured diffraction image of the object given by Eq. (5.3). The inversion algorithm was able to return reasonable answers as compared to the true values. We will not quote any of these results and go to the "noisy" measurement situation.

In Figure 2 we show a sample realization of the reconstruction in the presence of 2% measurement noise. Note the presence of negative values of the modulus at the edges of the object; however the photometry of the reconstruction follows the true object very well except at the edges. Two sample realizations of the reconstruction of the modulus of the object, in the presence of 3% measurement noise are shown in Figs. 3 and 4. Again note the unphysical negative values of the modulus at the edges of the object. Considering the fact that the object is so small, the modulus is in reasonable agreement with the true object in spite of measurement noise.

The troublesome feature of the present inversion algorithm is obviously the occurrence of negative modulus values at the edges of the object. The edges are somewhat unrealistic because they are of infinite slope and the algorithm tends to overshoot in the manner of a Gibbs phenomenon. We could, of course, consider objects with finite slopes at the edges to minimize the overshoots and undershoots; instead we have decided to develop a variant of the inversion algorithm using constrained minimization to surmount this annoying problem. Details will be reported in the near future.

6. SUMMARY

Given the rather discursive presentation, we feel it is useful to summarize the essentials of our approach to the problem. We consider the problem of determining the modulus and phase of the object at the lattice points as one of unconstrained minimization. A local (i.e., quadratic) model approach is used. We are in the fortunate position of employing both the Jacobian and Hessian, which, in the context of the discretized diffraction model, can be evaluated analytically! Thus we make use of both slope and curvature information, other methods only use slope information. The relatively new, and powerful trust region algorithm is then utilized in place of the usual line search algorithm. The trust region algorithm makes full use of the local model and takes into account local validity; moreover the algorithm exhibits global convergence properties.

REFERENCES

1 A.H. Bennett, H. Jupnik, H. Osterberg, and O.W. Richards, *Phase Contrast Microscopy* (Wiley, New York, 1951).

2 M. Pluta, *Advanced Light Microscopy*, vol. 2 (Elsevier, Amsterdam, 1988), Chpt. 5.

3 R. Barakat, "Diffraction images of coherently illuminated objects in the presence of aberrations," *Opt. Acta* 16, 205–223 (1969).

4 H. Stark (editor), *Image Recovery: Theory and Applications* (Academic, New York, 1987).

5 J. Fienup, "Reconstruction of an object from the modulus of its Fourier transforms," *Opt. Lett.* 3, 27–29 (1978).

6 J. Fienup, "Phase retrieval algorithms," *Appl. Opt.* 21, 2758–2769 (1982). Contains references to many of his previous papers on the Fienup algorithm.

7 R. Barakat and G. Newsam, "Algorithms for reconstruction of partially known, band-limited Fourier transform pairs from noisy data, I. The prototypical linear problem; II. The nonlinear problem of phase retrieval," *J. Integral Eqs.* 9, 49–125 (1985).

8 R. Barakat and G. Newsam, "Necessary conditions for a unique solution to two-dimensional phase retrieval," *J. Math. Phys.* 23, 3190–3193 (1984).

9 G. Newsam and R. Barakat, *Phase Retrieval in Two Dimensions*, Research Report CMA-R15–86, Australian National University Centre for Mathematical Analysis (Canberra, Australia, 1986).

10 N.E. Hurt, *Phase Retrieval and Zero Crossings* (Kluwer, Boston, 1989).

11 R. Barakat and B. Sandler, "Determination of the wavefront aberration function from measured values of the point spread function: A two-dimensional phase retrieval problem," *J. Opt. Soc. Am.*, Series A (in press).

12 A.N. Tichonov and V. Arsenin, *Solutions of Ill-Posed Problems* (Wiley, New York, 1977).

13 Y. A. Morozov, *Methods of Solving Incorrectly Posed Problems* (Springer Verlag, New York, 1984), Chapter 2.

14 J. Dennis and R. Schnable, *Numerical Methods for Unconstrained Optimization and Nonlinear Equations* (Prentice-Hall, Englewood Cliffs, NJ, 1983).

15 R. Fletcher, *Practical Methods of Optimization*, 2nd ed. (Wiley, New York, 1987).

16 J. J. More, "Recent developments in algorithms and software for trust region methods," in: *Mathematical Programming: The State of the Art*, eds. A. Bachem, M. Grotschel, and B. Korte (Springer-Verlag, Berlin, 1983), pp. 258–287.

FIGURE LEGENDS

Fig. 1 Distribution of illuminence in the diffraction image of a coherently illuminated opaque edge: $o(v) = 0$, $v < 0$ and $o(v) = 1$ for $v > 0$ viewed through an annular aperture of obscuration radius $\epsilon = 0.05$. The solid line is for the in-focus situation, the dotted line is for a half-wave of defocus. Taken from Reference 3.

Fig. 2 Sample realization of reconstruction of modulus and phase of coherently illuminated object (dashed lines) in the presence of 2% measurement "noise".

Fig. 3 Sample realization of reconstruction of modulus of coherently illuminated object (dashed line) in the presence of 3% measurement "noise".

Fig. 4 Sample realization of reconstruction of modulus of coherently illuminated object (dashed line) in the presence of 3% measurement "noise".

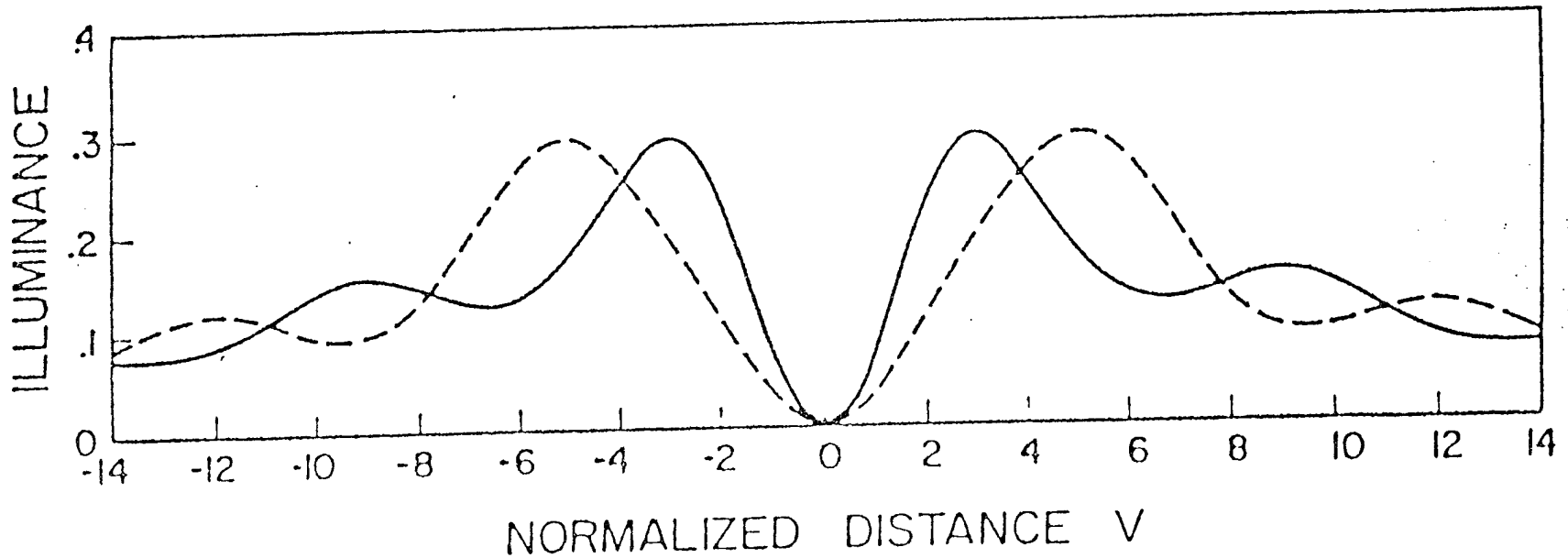
ILLUMINANCE
.4
.3
.2
.1
0
-14
-12
-10
-8
-6
-4
-2
0
2
4
6
8
10
12
14
NORMALIZED DISTANCE V

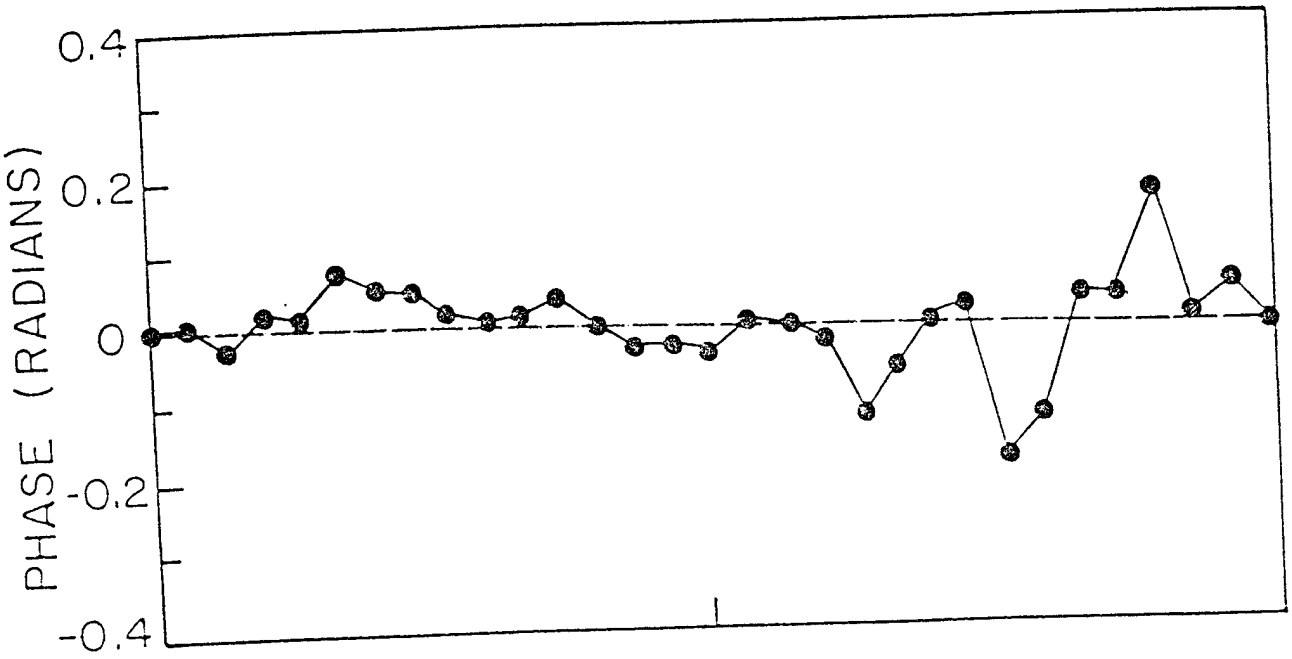

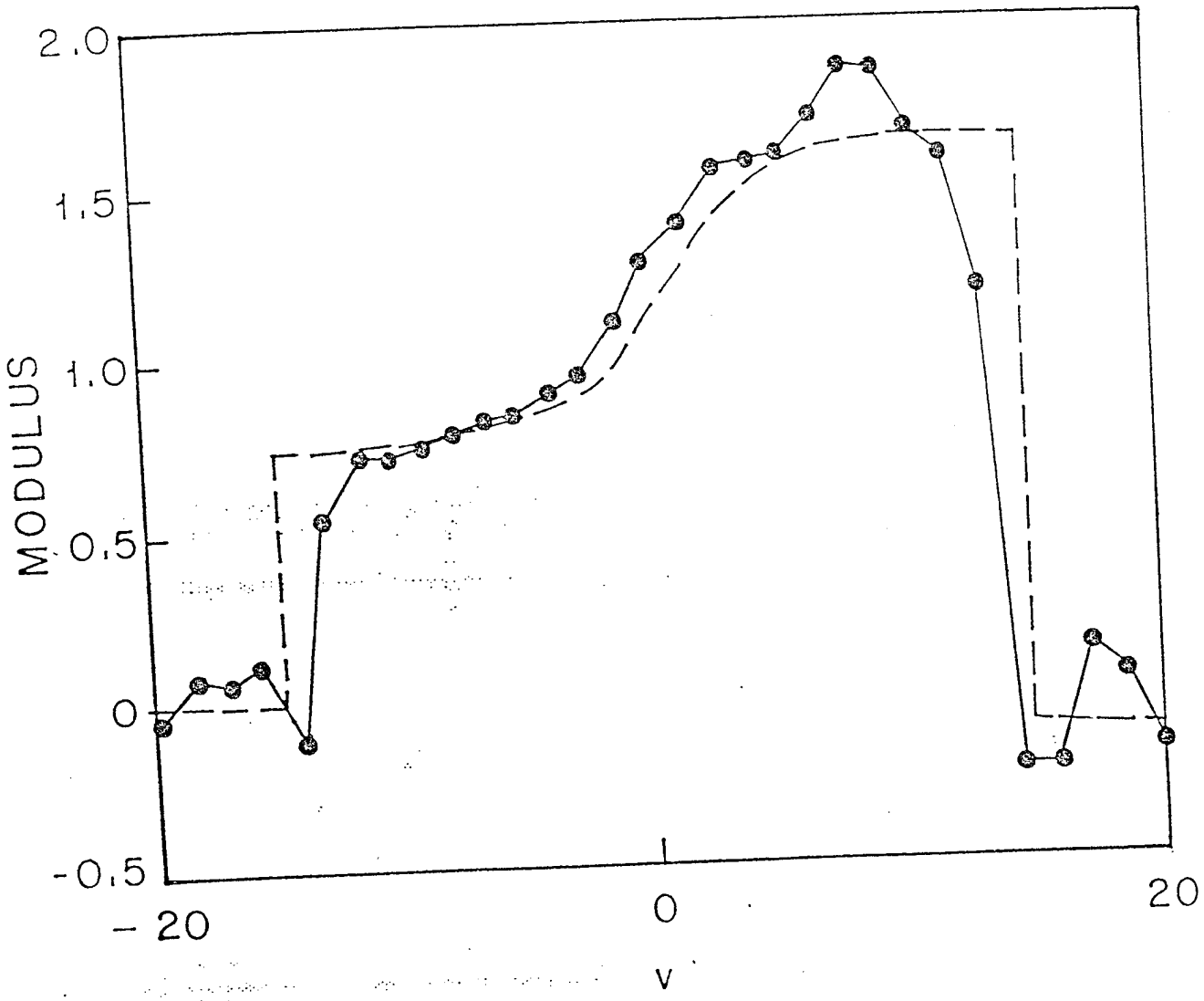

fig 2

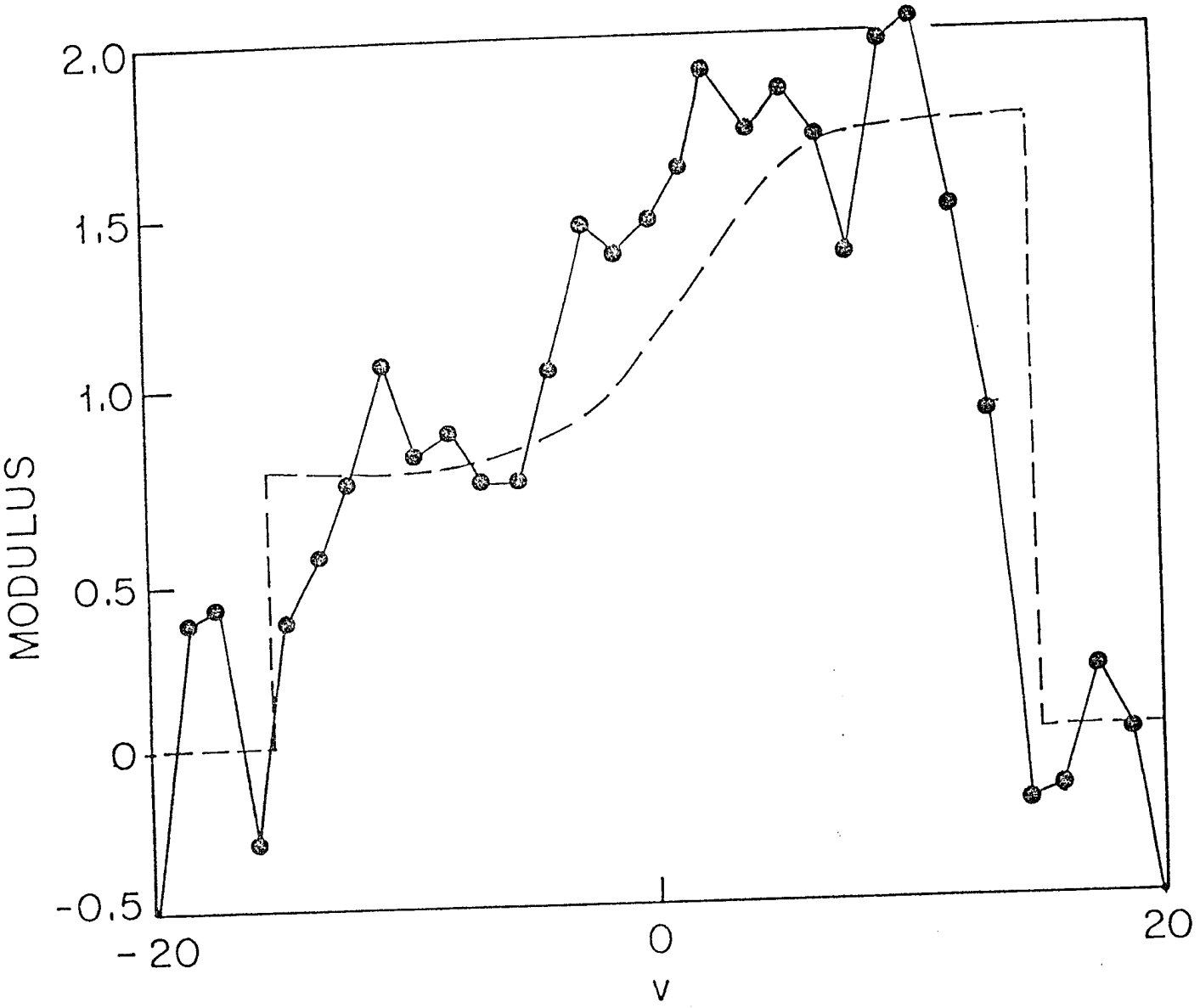
2.0
1.5
1.0
0.5
0
-0.5
MODULUS
-20
0
20
V

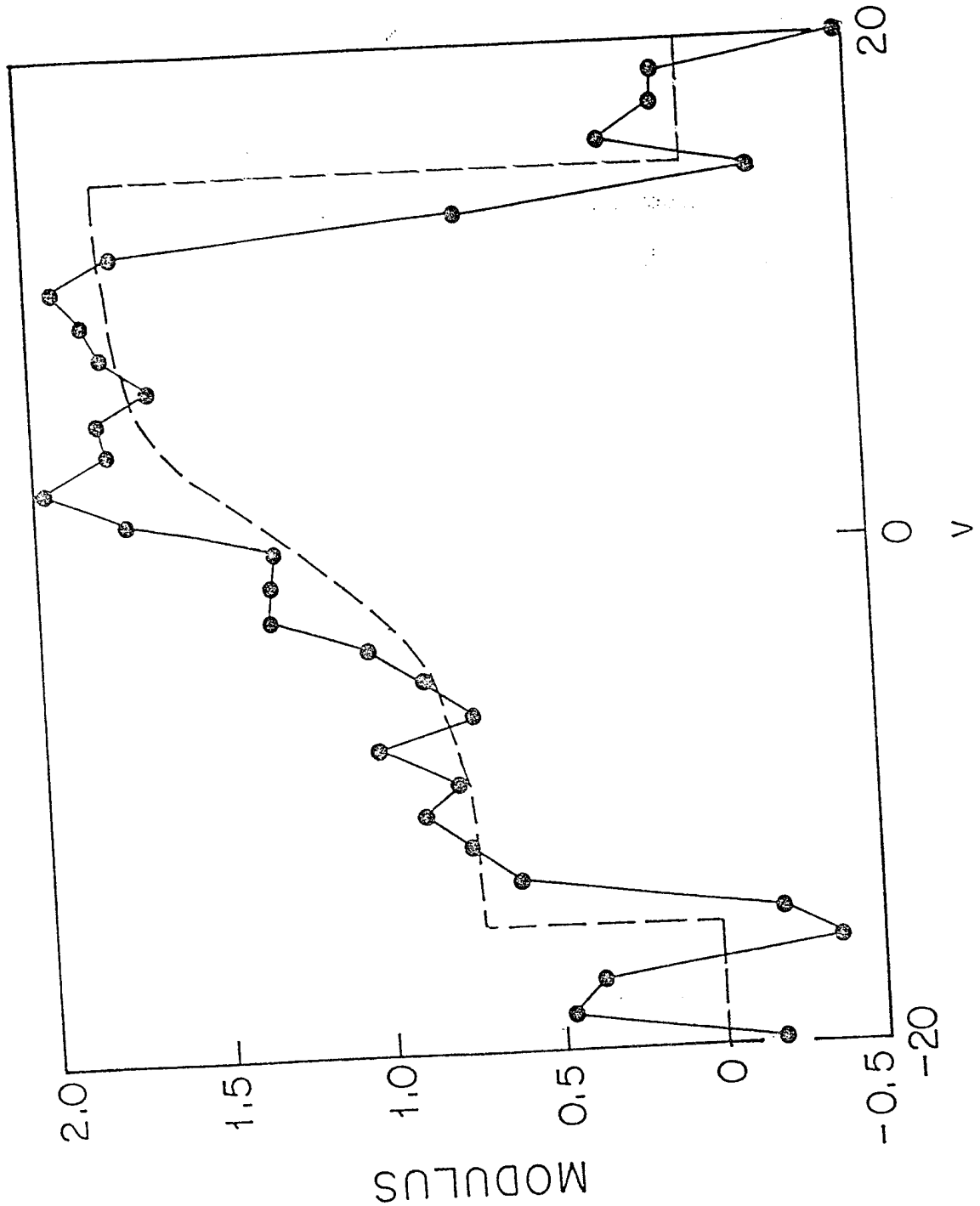

fig 4

LASER DOPPLER VELOCIMETRY ISSUES

The subject of laser doppler velocimetry (LDV) has been of interest to the Navy for many years and for a variety of reasons we need not chronicle. I have been tasked by Dr. William Statnick to investigate theoretical issues relating to this topic; this section contains some of my preliminary investigations into the subject, of which there are three subtopics reported at this time.

The first subtopic is devoted to the subject of increasing the signal-to-noise ratio in multichannel data for use in LDV. This I have accomplished by employing a deterministic version of the KL-expansion, the details are sketched out in the report. A second subtopic which arose from the first subtopic is that of determining a harmonic signal buried in Gaussian noise. While working on the deterministic KL-expansion, I figured a way to extend the stochastic KL-expansion to second order statistics. The work has been written for possible publication, and the details are given here in the form of a paper. The third subtopic is that of LDV itself.

SIGNAL-TO-NOISE ENHANCEMENT IN MULTICHANNEL DATA FOR USE IN LVD

Dr. William Statnick has raised the issue of understanding how to increase signal to noise ratios (SNR) in multichannel data for use in LDV, a very important topic with practical bearing. I have been able to develop an approach to the SNR enhancement problem using the Karhunen-Loeve transform. This approach will now be sketched; as noted in the introduction numerical computations were not attempted because of the necessity of having to use a parallel machine such as the CONNECTION machine or the PS-2 IBM machine (at MAUI). Hopefully if a follow-on is granted, then I intend to apply for time on the MAUI machine to perform the numerical calculations. The reason is quite simple, we need to look at as many of 200 channels in order to be realistic, serial machines are simply too slow. I doubt that a small number of channels (say 10 or 20) is of any real importance.

The basic idea behind my use of the KL expansion (or transform) is that it is the optimal way to extract coherent information from multichannel input data (such as is needed in some LDV scenarios) in a least squares norm sense. There are many ways to derive the KL expansion, but the present approach is probably the simplest for our purposes. A more mathematical approach using gap integral equations is discussed in the next subsection.

Suppose we have a set of n real signals (we could consider n complex signals, but the analysis becomes very elaborate without any additional insight). Call these signals $x_j(t)$ where j = 1,2,...,n. Define a transform $X_j(t)$ with an associated transformation matrix A (as yet undefined) such that

$$X_j(t) = \sum_{i=1}^{n} a_{ij} x_i(t)$$

where a_{ij} are the elements of matrix A. We want to choose the $X_j(t)$ such that they form an orthogonal basis, that is

$$x_i(t) = \sum_{j=1}^{n} b_{ij} X_j(t) , \qquad (i = 1,2,\cdots,n)$$

If the number of channels is very large, then we approximate the above by

$$y_i(t) = \sum_{j=1}^{m} b_{ij} X_j(t)$$

where $m < n$. How large m must be to approximate n can only be determined by numerical computation. The $y_i(t)$ are the reconstructed signals and b_{ij} are the matrix elements of B, the inverse expansion matrix.

Our object is to reconstruct the $x_j(t)$ using the smallest number of basis signals m, of course to some specified error. We choose (given a fixed m) to require that the matrices $\hat{\hat{A}}$ and $\hat{\hat{B}}$ are such that they minimize the least-squares error

$$e(m) = \sum_{i=1}^{n} \int_0^T \left[x_i(t) - y_i(t) \right]^2 dt$$

where T is the observation time.

It can be shown that the rows of the matrix $\hat{A}$ consist of the normalized eigenvectors of the matrix $\hat{C}$

$$c_{ij} \equiv \int_0^T x_i(t) x_j(t) dt$$

$\hat{C}$ is something like a covariance matrix, note that it is real, symmetric, and positive semi-definite; thus it possesses the decomposition

$$\hat{C} = \hat{U}\hat{S}\hat{U}^{+}$$

The matrix $\hat{U}$ contains the normalized eigenvectors $\hat{U}$; where

$$\hat{C}\hat{U}_j = \lambda_j \hat{U}_j$$

and $\hat{S}$ is a diagonal matrix of eigenvalues $(\lambda_1, \lambda_2, ..., \lambda_n)$. Note that these eigenvalues are nonnegative. When $\hat{A}=\hat{U}$, the rotated signals $X_j(t)$ form an n-dimensional subspace and we can show that the least-squares error is now given by

$$e(m) = \sum_{j=m+1}^{n} \lambda_j$$

Since the eigenvalues are arranged in descending order, it follows that the lower order basis functions can be used to reconstruct most of the signal (i.e., the lower order basis functions are somewhat like lower order Fourier basis functions).

We note the following, for our SNR application:

1. The KL-expansion produces a set of uncorrelated (or somewhat more precisely in the present context, orthogonal) basis functions from the data set.

2. The magnitude of the j-th eigenvalue is a measure of the amount of coherent energy present in the j-th basis function (for the proof see the appendix).

3. The fact in item 2 implies that the reconstructed signal using only the lower order basis functions amounts to reconstruction of the coherent energy present in the input.

I want to emphasize that this version of the KL-transform is deterministic in that the input signals are deterministic, whereas the analysis in the next subsection deals with the stochastic aspects of the KL-transform. In view of this difference, I suggest that a detailed numerical solution of both cases be carried out in order to determine which case really applies to the LDV scenario.

Appendix A

The energy of the basis functions can be studied thusly: Given the data vector $x(t) = \{x_i(t), i = 1,2,...,n\}$, compute the C matrix

$$\hat{C} = \hat{x}\hat{x}^{+}$$

Since $\hat{C}$ is symmetric, then

$$\hat{C} = \hat{U}\hat{\Lambda}\hat{U}^{+}$$

where $\hat{U}$ is the matrix of column eigenvectors $\hat{U}_j$ and $\hat{\Lambda}$ is the diagonal matrix of eigenvalues. Now $\hat{x}$ admits a singular value decomposition

$$\hat{x} = \hat{U}\hat{S}\hat{V}^{+}$$

where $\hat{\Lambda}$ is the matrix containing the singular values and $\hat{U}$, $\hat{V}$ are orthogonal matrices. It follows that

$$\hat{c} = \hat{U}\hat{S}\hat{V}^{+}\hat{V}\hat{S}^{+}\hat{V}^{+}$$
$$= \hat{U}\hat{S}\hat{S}^{+}\hat{V}^{+}$$

Next consider the basis function vector $\hat{\hat{X}} = \left\{\hat{X}_j(t): j = 1,2,\cdots,n\right\}$ which can be written as

$$\hat{X} = \hat{U}^{+}\hat{x}$$

We can easily show that

$$\begin{aligned}\hat{X}\hat{X}^{+} &= \hat{U}^{+}\hat{x}\hat{x}^{+}\hat{U} \\ &= \hat{S}\hat{S}^{+} = \hat{\Lambda}\end{aligned}$$

after some straightforward manipulations.

Additionally, we have

$$\begin{aligned}\mathrm{tr}\,\hat{\Lambda} &= \int_0^T \sum_{i=1}^{n} x_i^2(t)dt \\ &= \mathrm{tr}\,\hat{c}\end{aligned}$$

Comments

The above analysis permits us (at least in principle) to enhance SNR by orthogonal decomposition methods. Although succinctly stated, the numerical computations need to be carried out on a parallel machine to test the efficacy of the proposed method.

ABSTRACT

The statistics of a harmonic signal (coherent component) mixed with a random background (incoherent component) of a specified spectral profile (power spectrum) is still a problem of interest. The purpose of the present paper is to study the second-order intensity statistics of such a signal/background situation using the generalized Karhunen-Loevé expansion.

SECOND ORDER INTENSITY STATISTICS OF A COHERENT SIGNAL IN THE PRESENCE OF A RANDOM BACKGROUND

1. INTRODUCTION

In a classic paper written several years after the actual work (done during World War II), Kac and Siegert [1] determined the exact first-order statistics (i.e., probability density and moments) of a square law detector for a Gaussian random field, and for an harmonic signal buried in a Gaussian random field. Their approach involves the construction of a homogeneous integral equation whose kernel is the covariance function of the random field using what is now termed the Karhunen-Loevé expansion [2, 3], although we can also term the construction the Kac-Siegert expansion in as much as they derived it independently. The eigenvalues determine the probability density function of the detected intensity (square of the field amplitude), while both eigenvalues and eigenfunctions are needed for the probability density of the intensity of the signal and field. Emerson [4] also discusses the problem from an alternative viewpoint using the method of cumulants to avoid solving the associated homogeneous integral of Kac and Siegert. For further work on the problem, see Slepian [5]. As Mayer and Middleton [6] have pointed out, the original expansion method of Kac-Siegert is not general enough to handle higher-order statistics such as product moments. However, Kac-Siegert also present another method of solution, the "direct" method, which is capable of handling higher-order statistics. The direct method requires an appropriate transformation to express the output in terms of the input; the statistics of the output are then determined by suitable additional transformations with respect to the original input statistics. Mayer and Middleton exploit this approach to determine the higher-order statistics of the output due to a square law detector for both narrow-band and broad-band inputs. Kac-Siegert only consider the broad-band situation.

The purpose of the present paper is to restudy the above problems for the second-order intensity statistics using a generalization of the *original* Kac-Siegert expansion approach. I employ two point detectors to interrogate the random input (with and without the harmonic signal present). These detectors operate for the same time interval but are delayed

relative to each other by a variable time. The analysis is performed via an expansion of the random field over these two disjoint time intervals using a generalization of the Karhunen-Loevé series developed for similar problems in photon counting [7–9] and laser speckle [10]. In this approach, a homogeneous integral equation is constructed over the two *disjoint* time intervals wherein the two detectors operate. The eigenvalues and eigenfunctions (which obey an unusual orthogonality condition) are evaluated and used to fabricate a double generating function; from this double generating function the various product moments of the integrated intensities can be obtained by differentiation. The method can be carried out for the third order and higher statistics, see Blake and Barakat [11] for the third-order situation in the context of photon counting. Analysis is confined to the narrow-band situation, although there is no difficulty in studying the broad-band situation. I feel that the approach via the generalized Karhunen-Loevé expansion offers a more satisfying physical picture than the direct method in as much as the detector time intervals and delays are an inherent part of the analysis via the associated disjoint integral equation.

2. RANDOM INPUT FIELD

The complex-valued amplitude $U(t)$ of the total disturbance is the sum of a deterministic (or coherent) component $U_c(t)$ and a random background term $U_b(t)$

$$U(t) = U_c(t) + U_b(t) \, . \tag{2.1}$$

The coherent component is given by

$$U_c(t) = \xi_c e^{-i\omega_c t} \tag{2.2}$$

where ξ_c is a constant.

The random background $U_b(t)$ is taken to be a zero-mean, complex-valued, spatially stationary Gaussian random process, *i.e.*,

$$U_b(t) = U_b^{(r)}(t) + iU_b^{(i)}(t) \tag{2.3}$$

where $U_b^{(i)}(t)$ is the stochastic Hilbert transform of $U_b^{(r)}(t)$. Both $U_b^{(r)}$ and $U_b^{(i)}$ are real-valued. Now $U_b^{(r)}(t)$ and $U_b^{(i)}(t)$ have the same Gaussian probability density function (PDF) and are statistically independent. Furthermore

$$\langle U_b^{(r)}(t) \rangle = \langle U_b^{(i)}(t) \rangle = 0 \tag{2.4}$$

$$\langle U_b^{(r)}(t_1) U_b^{(r)}(t_2) \rangle = \langle U_b^{(i)}(t_1) U_b^{(i)}(t_2) \rangle = \frac{\sigma^2}{2} \, r_b(t_1 - t_2) \tag{2.5}$$

$$\langle U_b^{(r)}(t_1) U_b^{(i)}(t_2) \rangle \equiv 0 \tag{2.6}$$

where σ_b^2 is the variance of $U_b(t)$ and $r_b(t_1 - t_2)$ is the corresponding correlation function. $0 \leq |r_b| \leq 1$. Since $U_b(t)$ is a Gaussian random process, it is completely characterized by its mean, variance, and correlation function.

The disturbance $U(t)$ is interrogated by two-point detectors, the first detector operating during the time interval $(-T/2, T/2)$ and the second during the time interval $(\tau - T/2, \tau + T/2)$ where τ is the variable time delay. The integrated intensities Ω_j are

$$\begin{aligned} \Omega_1 &\equiv \int_{-T/2}^{T/2} |U(t)|^2 \, dt \\ \Omega_2 &\equiv \int_{\tau - T/2}^{\tau + T/2} |U(t)|^2 \, dt \quad . \end{aligned} \tag{2.7}$$

We can expand $U_b(t)$ in a generalized Karhunen-Loevé series [6–9] over the disjoint intervals

$$A_1 \equiv (-T/2, T/2), \qquad A_2 \equiv (\tau - T/2, \tau + T/2) \tag{2.8}$$

so that

$$\begin{aligned} U_b(t) &= \sum_{k=0}^{\infty} U_k \psi_k(t), \qquad t \in A_1 \quad \text{and} \quad A_2 \\ &= 0 \qquad\qquad , \qquad t \notin A_1 \quad \text{and} \quad A_2 \end{aligned} \quad . \tag{2.9}$$

The following conditions are to be satisfied:

1) The $\{U_k\}$ are random coefficients, independent of t; and are uncorrelated Gaussian random variables (hence, independent random variables)

$$\langle U_k U_\ell^* \rangle = \sigma_k^2 \delta_{k\ell} \tag{2.10}$$

where $\{\sigma_k\}$ are as yet unknown, real nonnegative constants. It is essential that $U(t)$ be Gaussian, for if it is not then the expansion coefficients $\{U_k\}$ will not be statistically independent, although they will still be uncorrelated.

2) The deterministic functions $\{\psi_k(t)\}$ are to form a complete orthonormal set over both A_1 and A_2.

The precise statement of the orthogonality condition is quite unusual. Consider the weighted sum of the integrated intensities: $\lambda_1\Omega_1^{(b)} + \lambda_2\Omega_2^{(b)}$ where λ_1, λ_2 are arbitrary real, nonnegative parameters appearing in the two-fold generating function of the integrated background intensities $\Omega_j^{(b)}$

$$Q_b(\lambda_1, \lambda_2) = \langle \exp(-\lambda_1\Omega_1^{(b)} - \lambda_2\Omega_2^{(b)}) \rangle \ . \tag{2.11}$$

As described in [7–9], we have

$$\lambda_1\Omega_1^{(b)} + \lambda_2\Omega_2^{(b)} = \sum_{k=0}^{\infty} |U_k|^2 \tag{2.12}$$

subject to the requirement

$$\oint \psi_k(t)\psi_\ell^*(t)\, dt = \delta_{k\ell} \tag{2.13}$$

where

$$\oint \equiv \lambda_1 \int_{-T/2}^{T-2} + \lambda_2 \int_{\tau-T/2}^{\tau+T/2} \ . \tag{2.14}$$

To evaluate the unknown constants σ_k in Eq. (2.10), we must construct an integral equation whose kernel is the correlation of function of $U_b(t)$. The integral equation is

$$\left(\lambda_1 \int_{-T/2}^{T-2} + \lambda_2 \int_{\tau-T/2}^{\tau+T/2} \right) r_b(t_1 - t_2)\psi_\ell(t_2)\, dt_2 = \left(\frac{\sigma_\ell}{\sigma}\right)^2 \psi_\ell(t_1) \ . \tag{2.15}$$

The correlation function $r_b(t_1 - t_2)$ of the random background field is given by

$$r_b(t_1 - t_2) = e^{i\omega_c(t_1 - t_2)} g_b(t_1 - t_2) \tag{2.16}$$

where $g_b(t_1 - t_2)$ is the correlation function centered at zero frequency and ω_0 is the frequency at which the power spectrum (lineshape) of the background radiation is a maximum. If we set

$$\phi_\ell(t) = \psi_\ell(t) e^{i\omega_0 t} \tag{2.17}$$

then Eq. (2.15) reads

$$\left(\lambda_1 \int_{-T/2}^{T-2} + \lambda_2 \int_{\tau-T/2}^{\tau+T/2} \right) g_b(t_1 - t_2) \phi_\ell(t_2)\, dt_2 = \left(\frac{\sigma_\ell}{\sigma} \right)^2 \phi_\ell(t_1) \tag{2.18}$$

independent of ω_0. This is the basic integral equation for determining $(\sigma_\ell/\sigma)^2$; it is not of the standard Fredholm type because of the presence of two disjoint domains of integration. A second difficulty is that the eigenvalues σ_ℓ^2 are implicit functions of λ_1 and λ_2.

The two-fold generating function $q_b(\lambda_1, \lambda_2)$ can be expressed as an infinite product. To prove this we note that from its definition, Eq. (2.11),

$$Q_b(\lambda_1, \lambda_2) = \int_0^\infty \cdots \int_0^\infty f[\{U_k\}] e^{-\lambda_1 \Omega_1^{(b)} - \lambda_2 \Omega_2^{(b)}} \prod_{k=0}^{\infty} d^2 U_k \tag{2.19}$$

where $d^2 U_k = dU_k^{(r)} dU_k^{(i)}$, and $f[\{U_k\}]$ is the joint probability density function of the statistically independent Gaussian random variables:

$$f[\{U_k\}] = \prod_{k=0}^{\infty} \frac{1}{\pi \sigma_k^2} e^{-|U_k|^2/\sigma_k^2} . \tag{2.20}$$

Upon substituting Eq. (2.15) into the integrand, we encounter a standard Gaussian integral. It can be shown [6–9] that

$$Q_b(\lambda_1, \lambda_2) = \prod_{k=0}^{\infty} [1 + \sigma_k^2(\lambda_1, \lambda_2)]^{-1} , \tag{2.21}$$

Thus far we have only considered the random background field $U_b(t)$. In the next section we will modify the analysis to include the coherent component (signal).

3. RANDOM INPUT FIELD WITH COHERENT SIGNAL

The starting point for the inclusion of the signal term, $U_c(t)$, is the double generating function as given in Eq. (2.19) with $\Omega_j^{(b)}$ replaced by Ω_j. In particular

$$\lambda_1\Omega_1 + \lambda_2\Omega_2 = \oint |U_b(t)|^2\, dt + \oint |U_c(t)|^2\, dt + \oint U_b(t)U_c^*(t)\, dt + \oint U_b^*(t)U_c(t)\, dt\,. \tag{3.1}$$

The first term on the right-hand side has already been evaluated, see Eq. (2.12); while the second term yields

$$\oint |U_c(t)|^2\, dt = 2|\xi_c|^2 T(\lambda_1 + \lambda_2)\,. \tag{3.2}$$

The interaction integrals (third and fourth terms) are

$$\begin{aligned} \oint U_b(t)U_c^*(t)\, dt &= \xi_c^* \sum_{k=0}^{\infty} U_k \oint \phi_\ell(t) e^{i\Delta t}\, dt \\ \oint U_b^*(t)U_c(t)\, dt &= \xi_c \sum_{k=0}^{\infty} U_k^* \oint \phi_\ell^*(t) e^{-i\Delta t}\, dt \end{aligned} \tag{3.3}$$

where

$$\Delta \equiv (\omega_c - \omega_0) \tag{3.4}$$

is the frequency offset describing the position of the signal with respect to the maximum of the background power spectrum.

Consequently Eq. (3.1) reduces to

$$\lambda_1\Omega_1 + \lambda_2\Omega_2 = \sum_{k=0}^{\infty} |U_k|^2 + 2|\xi_c|^2 T(\lambda_1 + \lambda_2) + \xi_c \sum_{k=0}^{\infty} U_k^* G_k(\lambda_1, \lambda_2) + \xi_c^* \sum_{k=0}^{\infty} U_k G_k^*(\lambda_1, \lambda_2) \tag{3.5}$$

where

$$G_k(\lambda_1, \lambda_2) \equiv \oint \phi_k(t) e^{i\Delta t}\, dt\ . \tag{3.6}$$

Given Eq. (3.5), we have

$$Q(\lambda_1, \lambda_2) = \exp\{-|\xi_c|^2 T(\lambda_1 + \lambda_2)\} \prod_{k=0}^{\infty} Q_k(\lambda_1, \lambda_2) \tag{3.7}$$

where

$$Q_k(\lambda_1, \lambda_2) \equiv \frac{1}{\pi\sigma_k^2} \int_{-\infty}^{\infty} e^{-(1+\sigma_k^{-2})|U_k|^2}\ e^{-\xi_q^* G_k^* U_k - \xi_q G_k U_k^*}\ d^2U_k\ . \tag{3.8}$$

To evaluate Q_k, we note that since $U_k = V_k + iW_k$, then

$$\xi_c^* G_k^* U_k + \xi_c G_k U_k^* = a_k V_k + i b_k W_k \tag{3.9}$$

where

$$\begin{aligned} a_k &= \xi_c^* G_k^* + \xi_c G_k \\ b_k &= \xi_c^* G_k^* - \xi_c G_k \end{aligned} \tag{3.10}$$

Consequently

$$Q_k = \frac{1}{\pi\sigma_k^2} \int_{-\infty}^{\infty} e^{-(1+\sigma_k^{-2})V_k^2 - a_k V_k}\, dV_k \int_{-\infty}^{\infty} e^{-(1+\sigma_k^{-2})W_k^2 - i b_k W_k}\, dW_k\ . \tag{3.11}$$

Both integrals are known:

$$\int_{-\infty}^{\infty} e^{-(1+\sigma_k^{-2})V_k^2 - a_k V_k}\, dV_k = \frac{\sqrt{\pi}}{\sqrt{(1+\sigma_k^{-2})}}\ \exp\left[\frac{a_k^2}{4(1+\sigma_k^{-2})}\right] \tag{3.12}$$

$$\int_{-\infty}^{\infty} e^{-(1+\sigma_k^{-2})W_k^2}\ \cos b_k W_k\, dW_k = \frac{\sqrt{\pi}}{\sqrt{(1+\sigma_k^{-2})}}\ \exp\left[\frac{a_k^2 - b_k^2}{4(1+\sigma_k^{-2})}\right) \tag{3.13}$$

and Eq. (3.11) reduces to

$$Q_k(\lambda_1, \lambda_2) = \frac{1}{(1+\sigma_k^2)} \exp\left[\frac{|\xi_c G_k|^2 \sigma_k^2}{(1+\sigma_k^2)}\right] \quad . \tag{3.14}$$

Thus the double generating function for the background/signal is

$$\begin{aligned} Q(\lambda_1, \lambda_2) &= \exp\{-|\xi_c|^2 T(\lambda_1 + \lambda_2)\} \cdot \prod_{k=0}^{\infty} (1+\sigma_k^2)^{-1} \cdot \prod_{k=0}^{\infty} \exp\left\{\frac{|\xi_c G_k|^2 \sigma_k^2}{(1+\sigma_k^2)}\right\} \\ &\equiv Q_c(\lambda_1, \lambda_2) Q_b(\lambda_1, \lambda_2) Q_{bc}(\lambda_1, \lambda_2) \end{aligned} \tag{3.15}$$

where Q_c, Q_b are the generating functions for the coherent, background components respectively and Q_{bc} is the generating function for the interaction between background and signal.

The product moments of the integrated intensities can be obtained by differentiation of $Q(\lambda_1, \lambda_2)$:

$$\langle \Omega_1^p \Omega_2^q \rangle = (-1)^{p+q} \frac{\partial^{p+q}}{\partial \lambda_1^p \partial \lambda_2^q} Q(\lambda_1, \lambda_2)|_{\lambda_1 = \lambda_2 = 0} \quad . \tag{3.16}$$

4. DOUBLE GENERATING FUNCTION: SMALL APERTURE REGIME

It should be obvious that the larger are the receiving apertures the greater is the smoothing of the field amplitudes. Consequently we want to use apertures as small as possible, and now assume that T is small compared to the distance over which the correlation function $g_b(t)$ decays to its e^{-1} value.

Under this condition only the $k = 0$ terms in Q_b and Q_{bc} contribute. With reference to [7–9] we have

$$\sigma_0^2(\lambda_1, \lambda_2) = \sigma^2 T(\lambda_1 + \lambda_2) + \sigma^4 T^2[1 - g^2(\tau)]\lambda_1\lambda_2 \quad . \tag{4.1}$$

This leaves only the G_0 function to evaluate. We apply the mean value approximation to evaluate the integrals in Eq. (3.6), thereby obtaining

$$G_0 = b(\lambda_1 T + \lambda_2 T e^{i\Delta r}) \tag{4.2}$$

where $\phi_0(0) = \phi_0(\tau) =$ constant ($\equiv b$). Note that $|G_0|^2$ is a quadratic function of λ_1 and λ_2. Thus we have

$$Q(\lambda_1, \lambda_2) = (1 + \sigma_0^2)^{-1} \exp\{-|\xi_c|^2 T(\lambda_1 + \lambda_2)\} \exp\left\{\frac{|\xi_c G_0|^2 \sigma_0^2}{(1 + \sigma_0^2)}\right\} \quad . \tag{4.3}$$

5. PRODUCT MOMENTS: BACKGROUND/SIGNAL

The product moments of the integrated intensities were obtained by differentiation of $Q(\lambda_1, \lambda_2)$, Eq. (4.3), according to Eq. (3.16): I employed the symbol manipulation program, SMP, using a VAX computer to effect the differentiations. The first few product moments are:

$$\langle \Omega_1 \rangle = \langle \Omega_2 \rangle = \sigma^2 + |\xi_c|^2 \tag{5.1}$$

$$\langle \Omega_1 \Omega_2 \rangle = \sigma^4[1 + g^2(\tau)] + 2\sigma^2|\xi_c|^2 + |\xi_c|^4 \tag{5.2}$$

$$\begin{aligned}\langle \Omega_1^2 \Omega_2 \rangle = \langle \Omega_1 \Omega_2^2 \rangle &= 2\sigma^6[1 + 2g^2(\tau)] \\ &+ \sigma^4|\xi_c|^2[4 + 2g^2(\tau) + b + 2b\cos\Delta\tau] + 3\sigma^2|\xi_c|^4 + |\xi_c|^6\end{aligned} \tag{5.3}$$

$$\begin{aligned}\langle \Omega_1^2 \Omega_2^2 \rangle = 4\sigma^8[1 &+ 4g^2(\tau) + g^4(\tau)] \\ &+ \sigma^6|\xi_c|^2\{4 + 8g^2(\tau)[1 + b\cos\Delta\tau] + 8b\} \\ &+ \sigma^4|\xi_c|^4[2 + g^2(\tau) + 4b + 8b\cos\Delta\tau] \\ &+ 4\sigma^2|\xi_c|^6 + |\xi_c|^8 \ .\end{aligned} \tag{5.4}$$

Note that the frequency offset Δ only appears in $\langle \Omega_1^2 \Omega_2 \rangle$ and $\langle \Omega_1^2 \Omega_2^2 \rangle$ and not in $\langle \Omega_1 \Omega_2 \rangle$.

In the homodyne case where the frequency of the signal coincides with the maximum of the power spectrum of the background, then Δ vanishes and the product moments then depend upon $g(\tau)$ only.

REFERENCES

1. M. Kac and A. Siegert, "On the theory of noise in radio receivers with square law detectors," *J. Appl. Phys.* 18, 383–397 (1947).

2. I. Selin, *Detection Theory* (Princeton University Press, Princeton, NJ, 1965), Chapter 3.

3. J. Thomas, *Statistical Communication Theory* (Wiley, New York, 1969), Chapter 6.

4. R. Emerson, "First probability densities for receivers with square law detectors," *J. Appl. Phys.*24, 1168–1176 (1953).

5. D. Slepian, "Fluctuations of random noise powers," *Bell System Tech. J.* 37, 163–(1958).

6. M. Mayer and D. Middleton, "On the distributions of signals and noise after rectification and filtering," *J. Appl. Phys.* 25, 1037–1052 (1954).

7. E. Jakeman, "Theory of optical spectroscopy by digital autocorrelation of photon counting fluctuations," *J. Phys.* A3, 201-215 (1970).

8. J. Blake and R. Barakat, "Two-fold photoelectron counting statistics: The clipped correlation function," *J. Phys.* 6A, 1196–1210 (1973).

9. R. Barakat and J. Blake, "Theory of photoelectron counting statistics, an essay," *Phys. Rep.* 60, 225–340 (1980).

10. R. Barakat and J. Blake, "Second order statistics of speckle patterns observed through finite-size scanning apertures," *J. Opt. Soc. Am.* 68, 1217–1224 (1978).

LDV AND TURBULENCE ISSUES

A considerable effort during this contract was devoted to the workings of LDV itself (as a measurement tool for turbulence). The basic paper in this area is

W. George and J. Lumley, "The laser-doppler velocimeter and its application to the measurement of turbulence", J. Fluid Mech., 60, 321-362 (1973).

The key issue is the measurement of the doppler shift on the frequency of the light scattered from small particles moving in the turbulent fluid. George and Lumley (as well as others since their work) have concentrated upon this doppler shift in instantaneous frequency by employing ideas from frequency modulation (FM) theory due to Wang:

J. Lawson and G. Uhlenbeck, *Threshold Signals*, (McGraw-Hill, New York, 1950) see chapter 13.

who investigated the unmodulated carrier plus noise case. Unfortunately this case yields a covariance function with an infinite variance (this being the cause of all the troubles in the George-Lumley approach).

I have initiated (and essentially carried out) the analysis when the Gaussian noise is broad-band (as in the turbulence situation). Unfortunately the analysis is much more complicated than in the narrow-band case involving many multiple integrals over Bessel functions (which reduce to simple expressions in the narrow-band case). The main point, however, is that in this case the covariance function has a finite variance.

Discussions with Barbara Sandler, who does most of my serious programming, have convinced me that about the only way to proceed is numerically. We have developed numerical integration schemes for other problems that can be used for the broad-band FM situation. Based

on these considerations, I have decided to postpone writing up this material until I begin numerical computations.